Antiviral Research 98 (2013) 332–343

Contents lists available at SciVerse ScienceDirect

Antiviral Research

journal homepage: www.elsevier.com/locate/antiviral

Lovastatin treatment mitigates the pro-inflammatory cytokine response in respiratory syncytial virus infected macrophage cells

Laxmi Iyer Ravi [a,1], Liang Li [b,1], Pui San Wong [c], Richard Sutejo [a], Boon Huan Tan [c], Richard J. Sugrue [a,b,*]

[a] Division of Molecular and Cell Biology, School of Biological Sciences, Nanyang Technological University, 60 Nanyang Drive, Singapore 637551, Singapore
[b] Singapore-MIT Alliance for Research & Technology (SMART), Centre for Life Sciences, 28 Medical Drive, Singapore 117456, Singapore
[c] Detection and Diagnostics Laboratory, DSO National Laboratories, 27 Medical Drive, Singapore 117510, Singapore

ARTICLE INFO

Article history:
Received 25 October 2012
Revised 1 March 2013
Accepted 9 March 2013
Available online 22 March 2013

Keywords:
Lovastatin
Pro-inflammatory cytokine
Respiratory syncytial virus
Macrophage

ABSTRACT

Disease severity following respiratory syncytial virus (RSV) infection is associated with inflammation due to enhanced pro-inflammatory cytokine secretion, and lung macrophage cells play a role in this process. In this study we evaluated the hydroxymethylglutaryl coenzyme A reductase inhibitor lovastatin as an anti-inflammatory drug to control RSV-induced cytokine secretion in the murine RAW 264.7 (RAW) macrophage cell line and in primary murine lung macrophages. These cells could be efficiently infected with RSV *in vitro*, and although no significant level of infectious virus particles were produced, the increased expression of several virus structural proteins could be detected. Virus infection and gene expression correlated with increased pro-inflammatory cytokine secretion by 24 h post infection. Lovastatin treatment did not reduce the cellular cholesterol levels in RSV-infected cells, nor did it inhibit RSV infection. However, we observed a significant reduction in the pro-inflammatory cytokine levels in lovastatin-treated RSV-infected cells. Since enhanced pro-inflammatory cytokine secretion is a major factor in RSV-associated pathology our findings highlighted the potential use of statins to mitigate and control the inflammatory response due to RSV infection. Furthermore, our study suggested that RAW cells maybe a simple and cost-effective model cell system to screen small molecule libraries to identify compounds that are effective in reducing RSV-induced inflammation.

1. Introduction

Human respiratory syncytial virus (RSV) is the most important cause of lower respiratory tract (LRT) infection in young children and neonates (Nair et al., 2010). RSV infection gives rise to a spectrum of clinical symptoms from relatively mild symptoms to severe bronchial pneumonia which can be fatal. This clinical scenario is worsened by the lack of an effective vaccine, and the limited availability of specific antivirus drugs to treat and prevent RSV infection. Disease severity is associated with inflammation due to enhanced pro-inflammatory cytokine secretion which can lead to extensive lung tissue damage. Therefore, regulating the host's pro-inflammatory response by using drugs that can suppress pro-inflammatory cytokine secretion may be a viable strategy to counter the immune pathology that is associated with RSV infection.

Hydroxymethylglutaryl coenzyme A reductase (HMGCR) is a key regulatory enzyme involved in endogenous cholesterol biosynthesis (Brown et al., 1973; Osborne et al., 1987). Cholesterol metabolism has also been implicated in inflammation, and statin-based drugs that inhibit HMGCR activity has been reported to reduce the expression of pro-inflammatory cytokines (Chaudhry et al., 2008; Ferro et al., 2000; Huang et al., 2003; Novack et al., 2009; Rezaie-Majd et al., 2002; Sakamoto et al., 2009). The murine animal model of RSV infection exhibits many of the features observed in the human disease (Johnson et al., 2007), and has been used in many studies to examine the pathology of RSV infection. RSV infection of pulmonary macrophages in severely infected patients has been demonstrated (Johnson et al., 2007), and lung macrophages are proposed to play an important role in the early response to RSV infection (Haeberle et al., 2002; Pribul et al., 2008; Reed et al., 2008). Statin-based drugs are effective in protecting mice from lethal RSV infection (Gower and Graham, 2001), but the basis for this observation was not defined. Given the importance that cytokine production plays in RSV-associated pathology (reviewed in Collins and Graham, 2008) we have used *in vitro* cell systems to examine if lovastatin was effective in reducing the pro-inflammatory response in RSV-infected macrophage cells.

* Corresponding author at: Division of Molecular and Cell Biology, School of Biological Sciences, Nanyang Technological University, 60 Nanyang Drive, Singapore 637551, Singapore.
E-mail address: rjsugrue@ntu.edu.sg (R.J. Sugrue).
[1] Equal contribution.

0166-3542/$ - see front matter © 2013 Elsevier B.V. All rights reserved.
http://dx.doi.org/10.1016/j.antiviral.2013.03.015

2. Materials and methods

2.1. Virus and tissue culture

The RSV A2 strain was prepared using HEp2 cell culture as described previously (Radhakrishnan et al., 2010). RSV infectivity was determined using the HEp2 cell microplaque assay (Cannon, 1987; Sugrue et al., 2001). Unless specified, cells were infected with RSV using a multiplicity of infection (moi) of three in DMEM + 2%FCS at 33 °C. RAW 264.7 (RAW) cells were maintained in minimum eagles medium and HEp2 cells were maintained in Dulbecco's Modified Eagle's medium (DMEM) (Gibco) containing 10% fetal bovine serum (FBS) and 1% penicillin/streptomycin (Gibco) at 37 °C in 5% CO_2. Murine lung CD11b+ cells were prepared from 6 to 8 weeks old special pathogen-free (SPF) female Balb/c mice as described previously (Perrone et al., 2008), but with modifications. The lungs were digested with collagenase D (1 mg/ml; Gibco) and single cell suspension (0.5% BSA, 2 mM EDTA, in 1XPBS). CD11b+ cells were purified using CD11b microbeads and a LS positive selection column (Miltenyi Biotec) and cultured in L929 cell conditioned (30%) medium at 37 °C in 5% CO_2. Prior to use in experiments the cells were washed briefly using PBS to remove non-adhered cells.

2.2. Ethical approval

This study was carried out in strict accordance with the recommendations in the guidelines on the care and use of animals for scientific purposes of the National Advisory Committee for Laboratory Animal Research (NACLAR), Singapore. The protocol was approved by the Institutional Animal Care and Use Committee, National University of Singapore (Approved Protocol Number: 046/09). All the operations on animals were done after the euthanasia of the animals by CO_2 inhalation, and all efforts were made to minimize animal suffering.

2.3. Antibodies and specific reagents

The F protein (MAb 19), N protein and M2-1 protein antibodies have been described previously (McDonald et al., 2004). The G protein, LAMP1 and LAMP2 antibodies were purchased from Abcam, anti-RSV (RCL3) was purchased from Novacastra Laboratories, and anti-actin was purchased from Sigma Aldrich. The mouse and rabbit secondary antibodies were purchased from Molecular Probes. Lovastatin (Calbiochem) was activated prior to use as described previously (Keyomarsi et al., 1991), and cells were pretreated with activated lovastatin (10 μM in DMEM) for 12 h prior to infection (Gower and Graham, 2001).

2.4. Immunofluorescence microscopy

Cells were fixed with 3% paraformaldehyde (PFA) in PBS for 30 min at 4 °C, permeabilized using 0.1% triton X100, and labelled using appropriate primary and secondary antibodies as described previously (McDonald et al., 2004). The stained cells were visualized using either a Nikon eclipse 80i fluorescence microscope or a Zeiss Axioplan 2 confocal microscope using appropriate machine settings.

2.5. Scanning electron microscopy (SEM)

Cells grown on glass coverslips were critically point dried (Polaron CPD) prior to mounting on aluminium stubs and carbon coated using an Edwards sputter coater device (Jeffree et al., 2003). The cells were visualized using a Jeol 5600 using appropriate machine settings.

2.6. Surface protein labelling

This was performed as described previously (Low et al., 2008). Briefly, cell monolayers were incubated with 0.5 mg/ml sulpho-NHS-LC-LC-biotin (Pierce). Biotinylated proteins were immunoprecipitated using anti-F and anti-G, and transferred onto PVDF membranes by Western blotting. The membranes were probed using streptavidin-HRP and protein bands detected using the ECL protein detection system (Amersham, USA).

2.7. Western blotting

The protein samples were transferred by western blotting onto PVDF membrane, which were blocked with PBS containing 5%(w/v) milk powder (Marvel™) as described previously (McDonald et al., 2004). The membrane was incubated with the appropriate primary antibody and anti-mouse IgG (whole molecule) peroxidase conjugate (Sigma, USA). The protein bands were visualized using the ECL protein detection system (Amersham, USA), and the apparent molecular masses were estimated using Kaleidoscope protein standards (Bio Rad, USA).

2.8. Cytotoxicity and cholesterol measurements

Cytotoxicity measurements were performed using the cytotoxicity detection kit, LDH ver 8 (Roche). The LDH levels were measured in the clarified tissue culture supernatant from non-treated and drug-treated cells (5×10^6 cells) as recommended by the manufacturer. Cholesterol levels were quantified from non-treated and drug-treated cells (5×10^6 cells) using the Amplex red cholesterol assay (Invitrogen) as recommended by the manufacturer. In both cases absorbance values were measured using a Tecan Infinite F200 microplate reader with i-Control software and using appropriate machine settings and wavelengths.

2.9. Cytokine assay

Tissue culture supernatants were centrifuged at 10,000*g* for 10 min at 4 °C after which the supernatant was used in the cytokine assay according to the manufacturer's instructions. Cytokines present in the media were analysed with the Bio-Plex Protein Array System (BioRad) using the Bio-Plex Mouse Cytokine 23-Plex Panel (1×96-well, # M60009RDPD, Bio-Rad).

2.10. PCR array

The extracted RNA from harvested cells was reverse transcribed using the RT^2 First Strand Kit (SABiosciences, USA) according to the manufacturer's protocol. For each 96-well plate, 1.0 μg of extracted RNA was used. The cDNA were then pre-mixed with RT^2 Real Time™ SYBR Green/Fluorescein PCR Master Mix, and applied on RT^2 Profiler PCR Array Mouse Inflammatory Cytokines & Receptors plates (SABiosciences, USA). The quantitative RT-PCR was run on the Applied Biosystems 7500 Fast Real Time PCR system (Applied Biosystems, USA) using appropriate settings. The threshold cycle (C_T) value was determined by standard setting in Applied Biosystems 7500 Fast Real Time PCR system as recommended by manufacturer. The fold-change was calculated by $2^{-\Delta\Delta CT}$ method with the software available at http://www.sabiosciences.com/pcrarraydataanalysis.php.

3. Results and discussion

3.1. RSV exhibits an abortive Infection in RAW264.7 cells

Low passage RAW 264.7 (RAW) murine macrophage cells were infected with RSV and at 24 hpi the cells were stained using anti-RSV (a composite antibody that recognises the N, P and M2-1 proteins). Examination by immunofluorescence (IF) microscopy indicated virus antigen was present in >95% of the infected cells (Fig. 1A). Virus-infected RAW cells were stained using antibodies against the F and the G virus surface glycoproteins, which revealed a punctate staining pattern on infected cells (Fig. 1B). Analysis by SEM showed evidence of membrane ruffling of the surface of mock-infected cells which increased following RSV infection (Fig. 1C). However, this morphology was distinct from the infectious virus filaments that form on RSV-infected epithelial cells where the virus matures as prominent finger-like projections that are up to 6 μm in length (Jeffree et al., 2003). The polymerase-associated proteins (N, P and M2-1 proteins) form cytoplasmic inclusion bodies in infected epithelial cells (Garcia et al., 1993), and anti-M2-1 and anti-RSV stained RAW cells revealed similar structures (Fig. 1B, highlighted by IB).

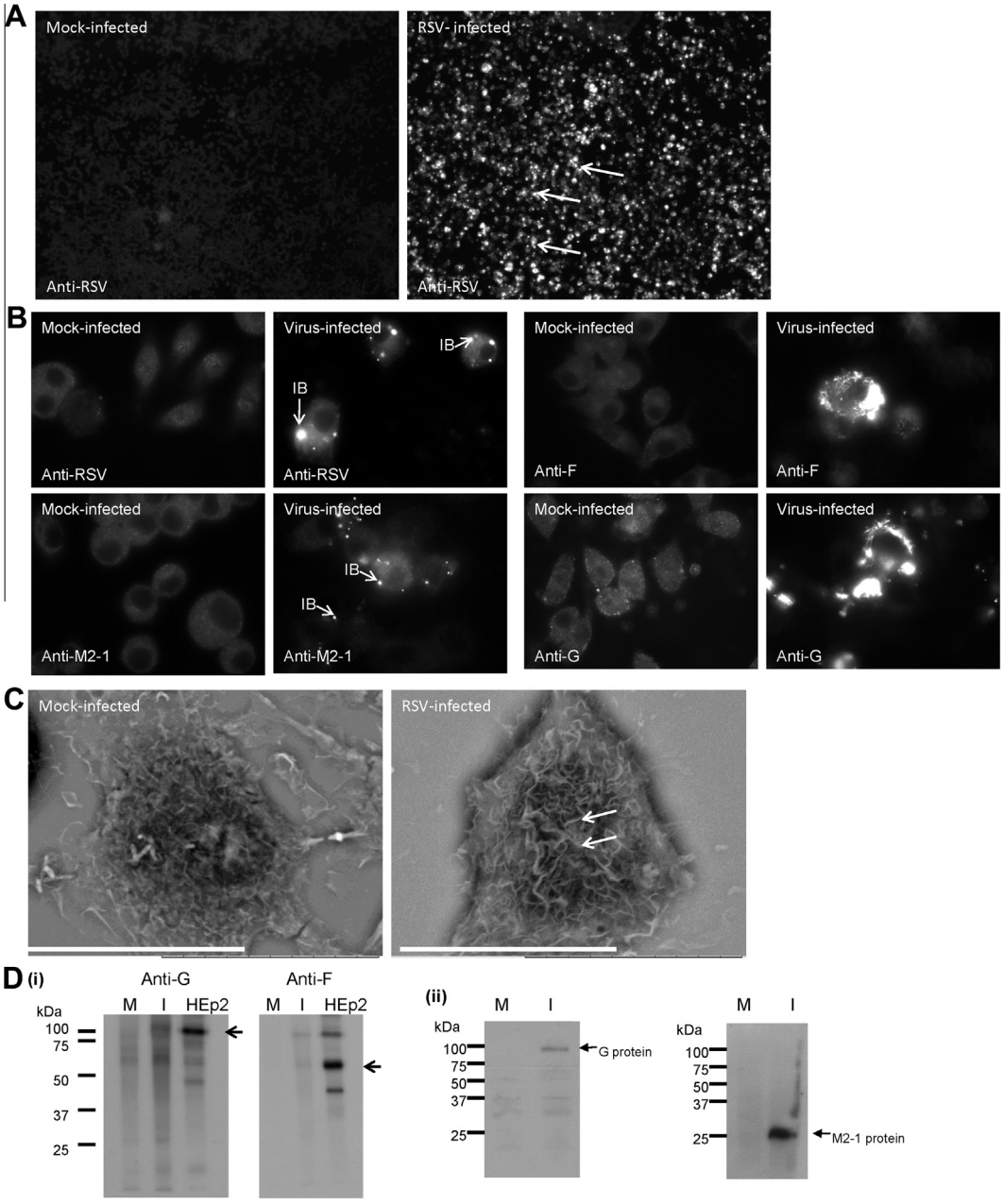

Fig. 1. Detection of RSV proteins in virus-infected RAW cells. (A) Mock-infected and RSV-infected RAW cells were fixed at 24 h post-infection (hpi) and stained with anti-RSV. Infected cells (highlighted by white arrows) were imaged using immunofluorescence microscopy (objective × 10). (B) Mock and RSV-infected cells were fixed at 24 hpi and stained with anti-F, anti-G, anti-RSV, or anti-M2-1 and analysed using fluorescence scanning confocal microscopy (objective × 63). The inclusion bodies (IB) are highlighted. (C) Scanning electron microscope analysis of mock-infected and RSV-infected RAW cells, increased surface membrane ruffling on virus-infected cells is highlighted (white arrows). White bar = 5 μm (D) (i) Surface expression of F and G glycoproteins. RAW cells were mock-infected (M) or RSV-infected (I) and at 24 hpi the cells were surface-biotinylated and the F and G protein immunoprecipitated using anti-F and anti-G respectively. A similar analysis was performed in parallel on HEp2 cells (HEp2). In all biotinylation assays 2×10^6 cells were used, and protein bands corresponding in size to the mature G and F1 proteins are indicated (black arrow). (ii) Immunoblot analysis of lysates prepared from mock-infected (M) and RSV-infected (I) RAW cells probed using anti-G and anti-M2-1.

We failed to detect the presence of the mature F and G glycoproteins on the surface of infected RAW cells, although in a parallel analysis both proteins could be readily detected on virus-infected HEp2 cells (Fig. 1D (i)). In comparison immunoblotting of infected RAW cell lysates using anti-G revealed a 90 kDa protein, which is the expected size for the mature G. This indicated that although the mature virus G protein was expressed in infected RAW cells, it was not displayed on the surface of infected cells. Immunoblotting of infected cell lysates with anti-M2-1 revealed a 22 kDa protein species which is the expected size of the M2-1 protein (Fig. 1D (ii)).

The imaging data suggested inefficient production of infectious virus particles in virus-infected RAW cells and this was examined further. HEp2 cells are highly permissive to RSV infection and produce relatively large quantities of infectious virus. Similar HEp2 and RAW cell numbers ($2x10^6$ cells) were infected with RSV using a moi of 0.1 and at 4 and 24 hpi the virus titres estimated and compared by microplaque assay (Sugrue et al, 2001). At 24 hpi a virus titer of 3×10^6 pfu/ml and 8×10^4 pfu/ml was recovered from the RSV-infected HEp2 and RAW cells respectively. At 4 hpi (i.e. soon after infection) a virus titre of 5.3×10^4 pfu/ml and 7.2×10^4 pfu/ml was measured in HEp2 cells and RAW cells, respectively, suggesting that the infectious virus measured in RAW cells at 24 hpi was largely due to the detection of residual virus from the virus inoculum.

The low efficiency of mature infectious virus production was confirmed by examining the virus transmission in RAW cells. Cells were infected with RSV using a moi of 0.05 and between 12 and 48 hpi the cells were stained using anti-RSV (Fig. 2A). Similar numbers of stained cells were observed at each time point, but the cells at the later time points showed significantly more intense labelling. The increased staining observed at 48 hpi was consistent with the presence of enlarged cytoplasmic inclusion bodies. Infected RAW cells were co-stained with anti-RSV, and either anti-LAMP1 or anti-LAMP2 (Fig. 2B and C) which recognise the two mature phagosomes cell marker proteins LAMP1 and LAMP2 respectively. Neither Anti-LAMP1 nor anti-LAMP2 co-localised with these

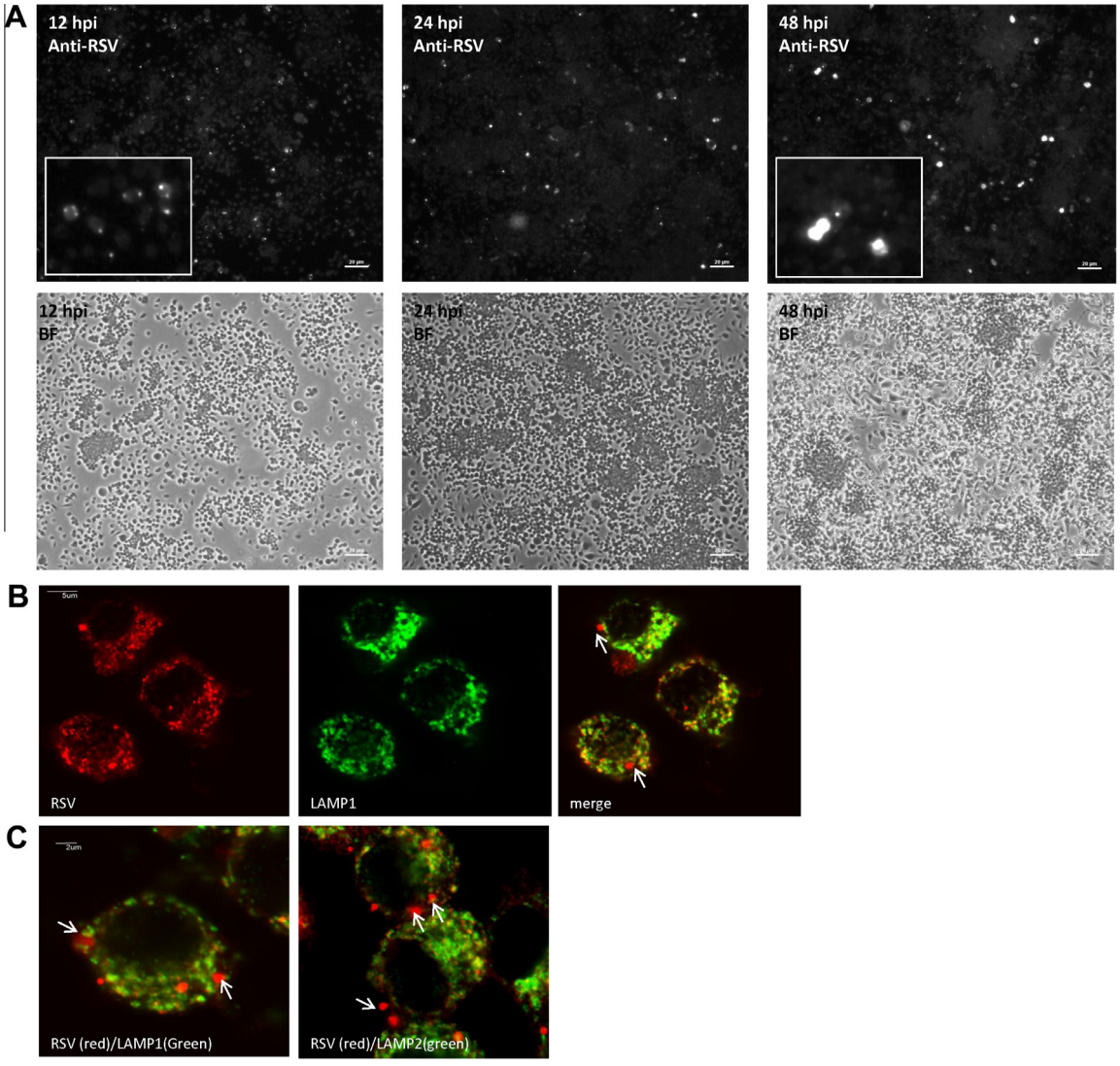

Fig. 2. Virus transmission does not occur in RSV-infected RAW cells. (A) Virus transmission does not occur in RSV-infected RAW cells. RAW cells were infected using a multiplicity of infection (moi) of 0.05 and at between 12 and 48 h post-infection (hpi) the cells were fixed and stained using anti-RSV. Inset, enlarged image showing infected cells in the monolayer are highlighted (white arrow). The same area of cells was imaged using fluorescence microscopy (anti-RSV) and bright field (BF) microscopy (objective × 10). In all cases identical camera settings were used. (B and C) RAW cells were infected with RSV and at 24 hpi the cells were stained using anti-RSV and anti-LAMP-1, or anti-RSV and anti-LAMP-2. The stained cells were visualised by fluorescence scanning confocal microscopy at (B) (objective × 40) and (C) at (objective × 100). The presence of virus inclusion bodies (white arrow) is highlighted.

A

GeneBank	Symbol	2 hpi Fold-change	16 hpi Fold-change
NM_011333	Ccl2/MCP-1	**4.8**	**7.0**
NM_013652	Ccl4/MIP-1β	**12.7**	**32.4**
NM_013653	Ccl5/RANTES	NC	**30.8**
NM_021274	Cxcl10/iP-10	**3.2**	**294.4**
NM_008176	Cxcl1/KC	2.3	**7.0**
NM_009971	Csf3	NC	**9678.9**
NM_008361	Il1β	NC	**3034.2**
NM_031168	Il6	2.5	**331.5**
NM_013693	Tnf	2.9	**44.6**

B

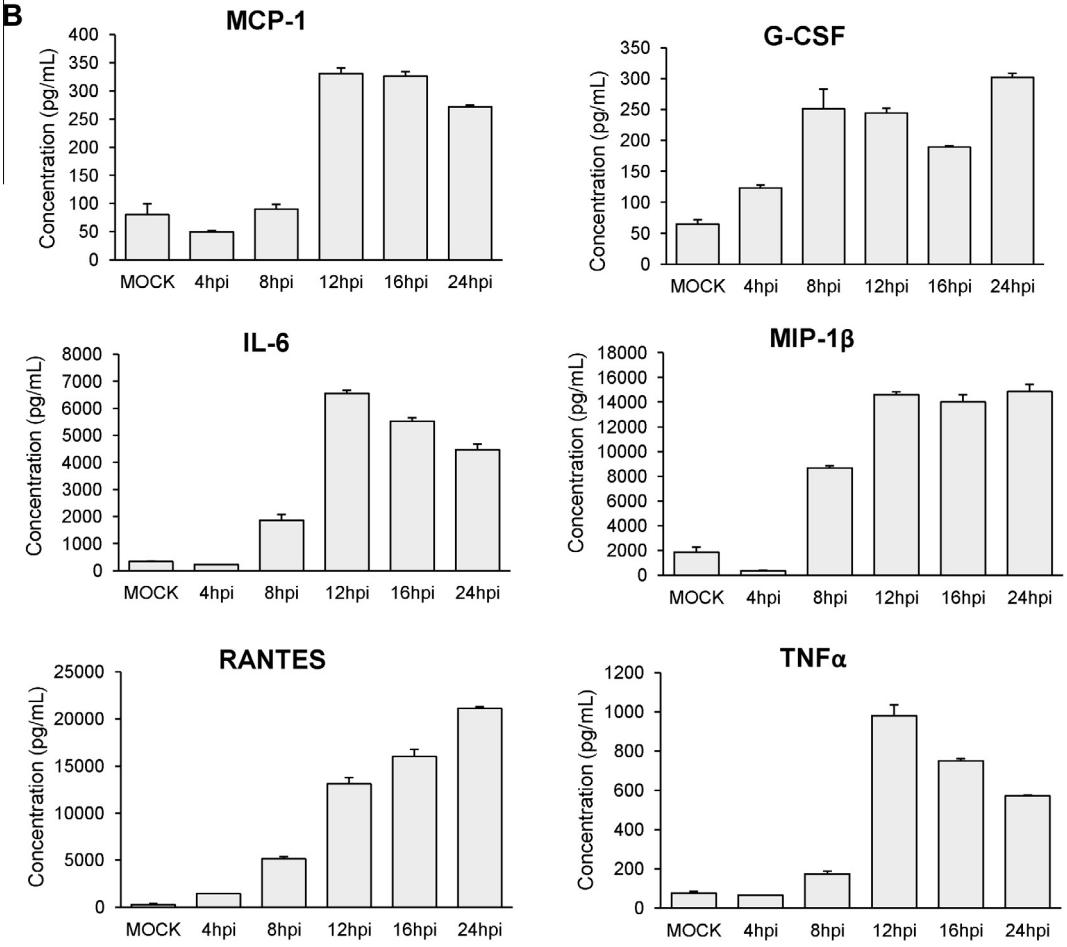

Fig. 3. Increased cytokine gene expression and cytokine secretion in RSV-infected RAW cells. (A) Effect of RSV infection on the expression of host-response genes in RSV-infected RAW cells using qPCR. At 2 h post-infection (hpi) and 16 hpi the relative fold-change (FC) in cytokine-related genes in virus-infected cells compared to that in mock-infected cells was measured by PCR array. Average values from three measurements are shown ($p < 0.05$). NC indicates no detectable change. (B) The cytokine concentrations in the tissue culture supernatant of mock-infected (24 hpi) and virus-infected RAW cells at between 4 and 24 hpi were measured using the Bio-Plex Mouse Cytokine 23-Plex Panel assay. Representative data from one of two independent experiments is presented, and the average values and standard error obtained from triplicate measurements are shown ($p < 0.05$).

structures indicating that the anti-RSV staining pattern was due to the presence of inclusion bodies and did not arise by engulfment of virus antigen in phagosomes.

Collectively these data indicate that although virus protein expression occurred in the infected RAW cells, significant virus transmission to neighbouring non-infected cells did not occur. This

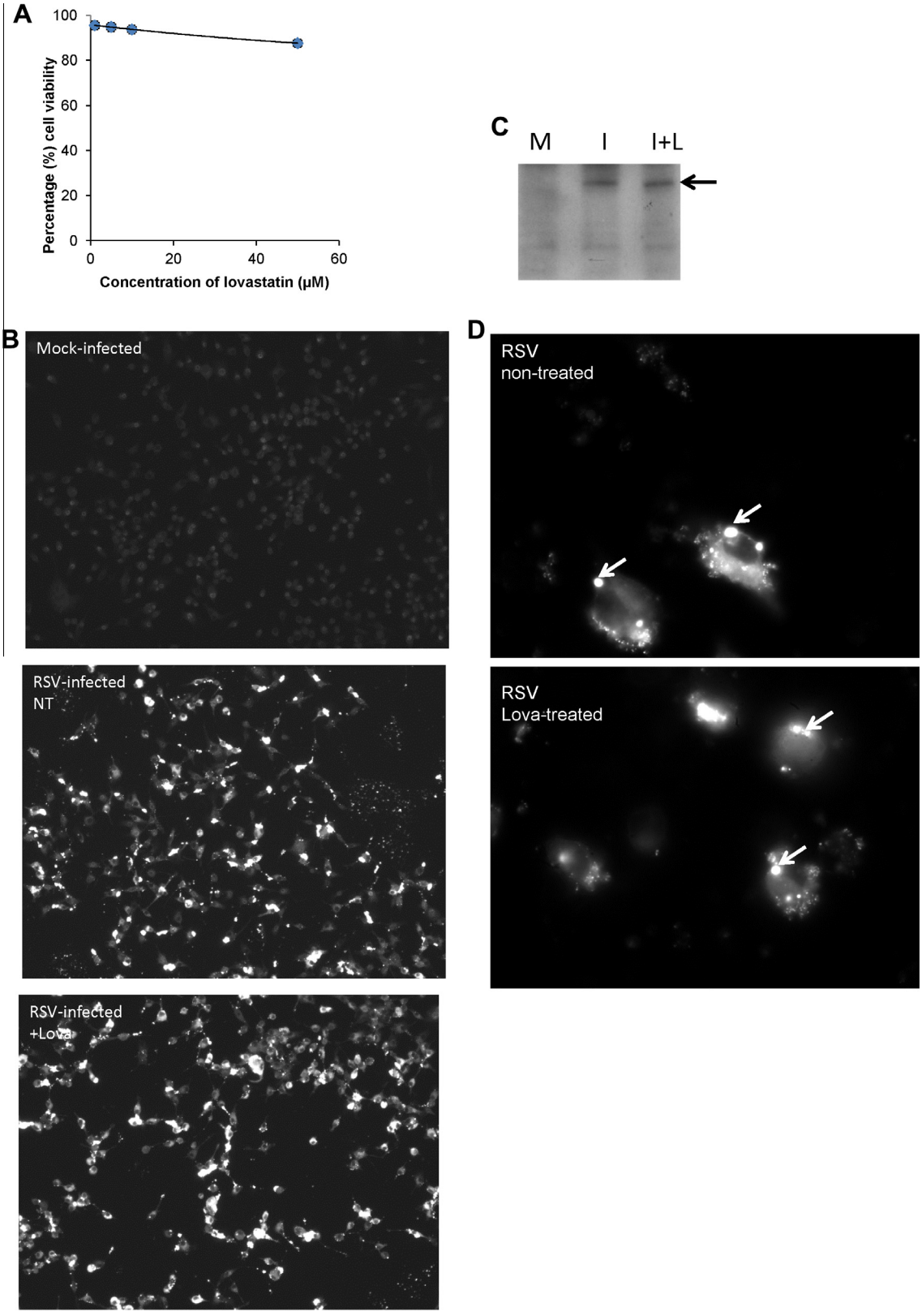

Fig. 4. The effect of lovastatin treatment on virus infection. (A) Mock-infected RAW cells were incubated with increasing lovastatin concentrations for 28 h and the cell viability measured. Representative data from one of two independent experiments is presented, and the average values and standard error obtained from triplicate measurements ($p < 0.05$) are shown. (B) RSV infection in RAW cells is not inhibited by lovastatin treatment. RAW cells were either mock-infected, or RSV-infected and either non-treated (NT) or lovastatin-treated (+Lova). At 24 h post-infection (hpi) the cells stained using anti-RSV and imaged using fluorescence microscopy (objective × 20). (C) At 24 hpi total cell lysates were prepared from mock-infected cells (M) and RSV-infected cells that were either non-treated (I) or lovastatin-treated (I+Lova). Lysates were transferred by Western blotting onto PVDF membranes and probed using anti-M2-1. A protein band corresponding in size to the M2-1 protein is indicated (black arrow). (D) Non-treated and lovastatin virus infected cells were stained using anti-RSV and imaged using fluorescence microscopy (objective × 100). Ther presence of inclusion bodies in infected cells is indicated (white arrows).

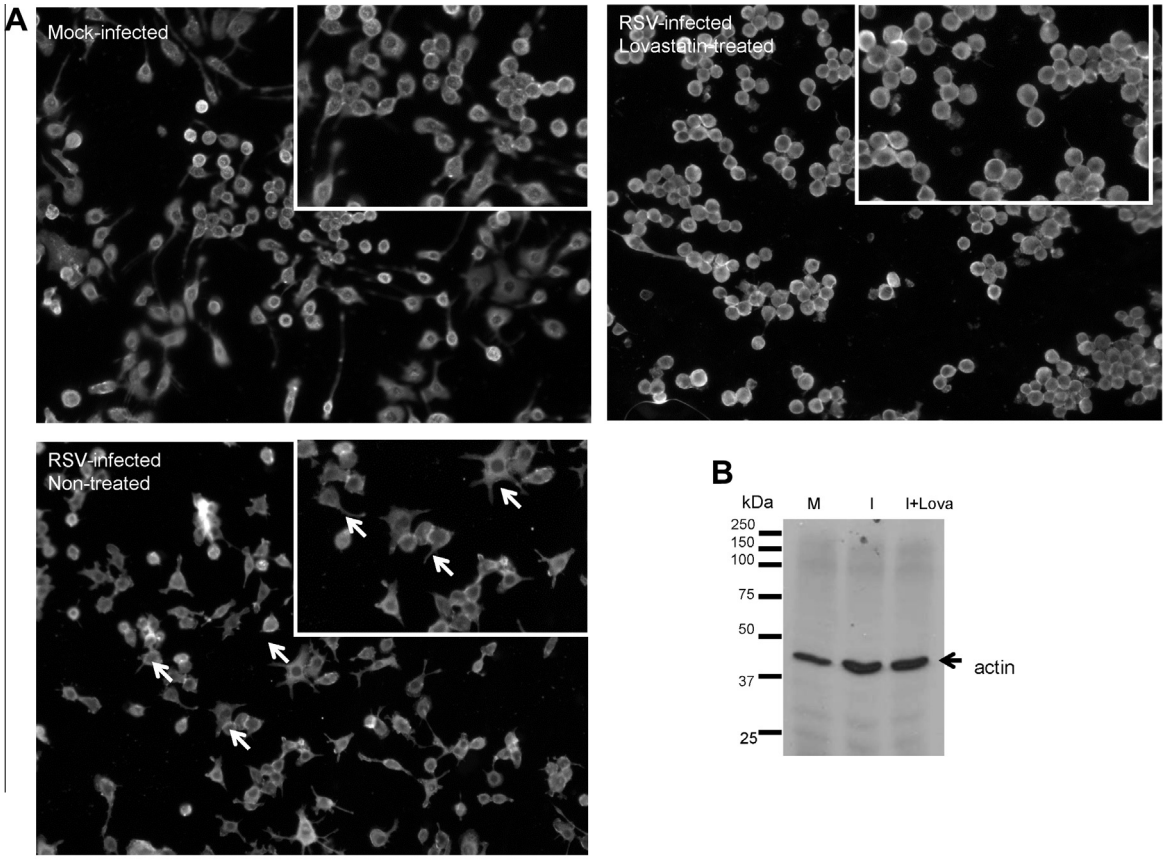

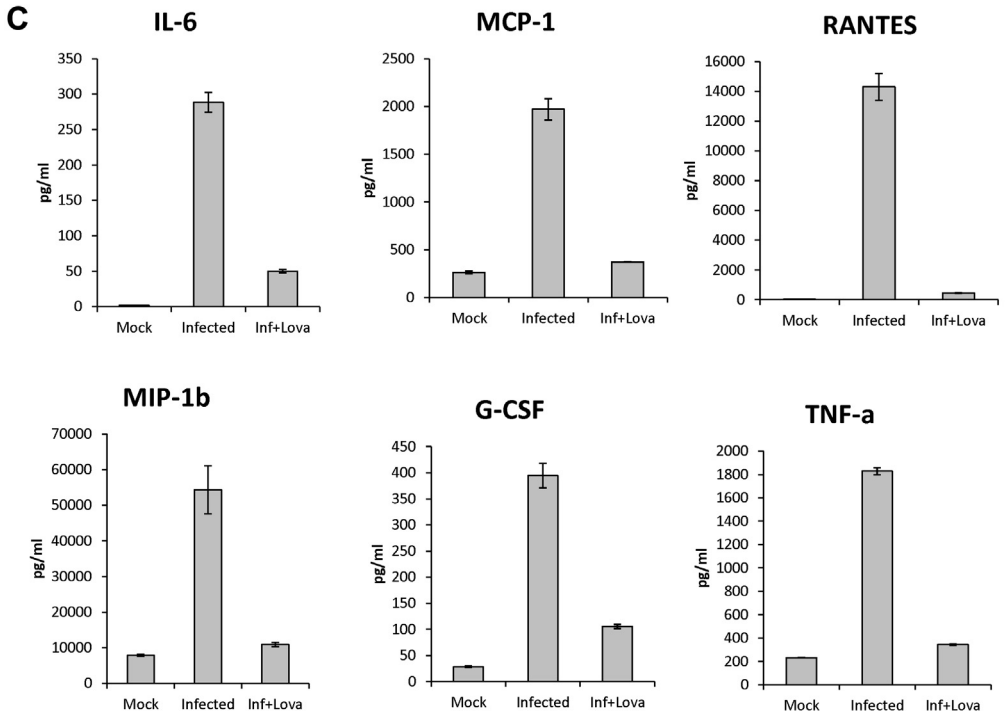

Fig. 5. The effect of lovastatin treatment on pro-inflammatory cytokine secretion in RSV-infected RAW cells. (A) Mock-infected cells and non-treated and lovastatin-treated RSV-infected cells were stained using phalloidin-FITC and imaged using fluorescence microscopy (objective ×20). Inset shows enlarge image of cells showing change in F-actin staining in RSV infection (highlighted by white arrow). (B) At 24 hpi total cell lysates were prepared from mock-infected cells (M) and RSV-infected cells that were either non-treated (I) or lovastatin-treated (I+Lova). Lysates were transferred by Western blotting onto PVDF membranes and probed using anti-actin. A protein band corresponding in size to the actin protein is indicated (black arrow). (C) The tissue culture supernatant was harvested from mock-infected and non-treated or lovastatin-treated RSV-infected cells at 24 hpi. The cytokine levels were measured using the Bio-Plex Mouse Cytokine 23-Plex Panel assay. Representative data from one of two independent experiments is presented, and the average values and standard error obtained from triplicate measurements ($p < 0.05$) are shown.

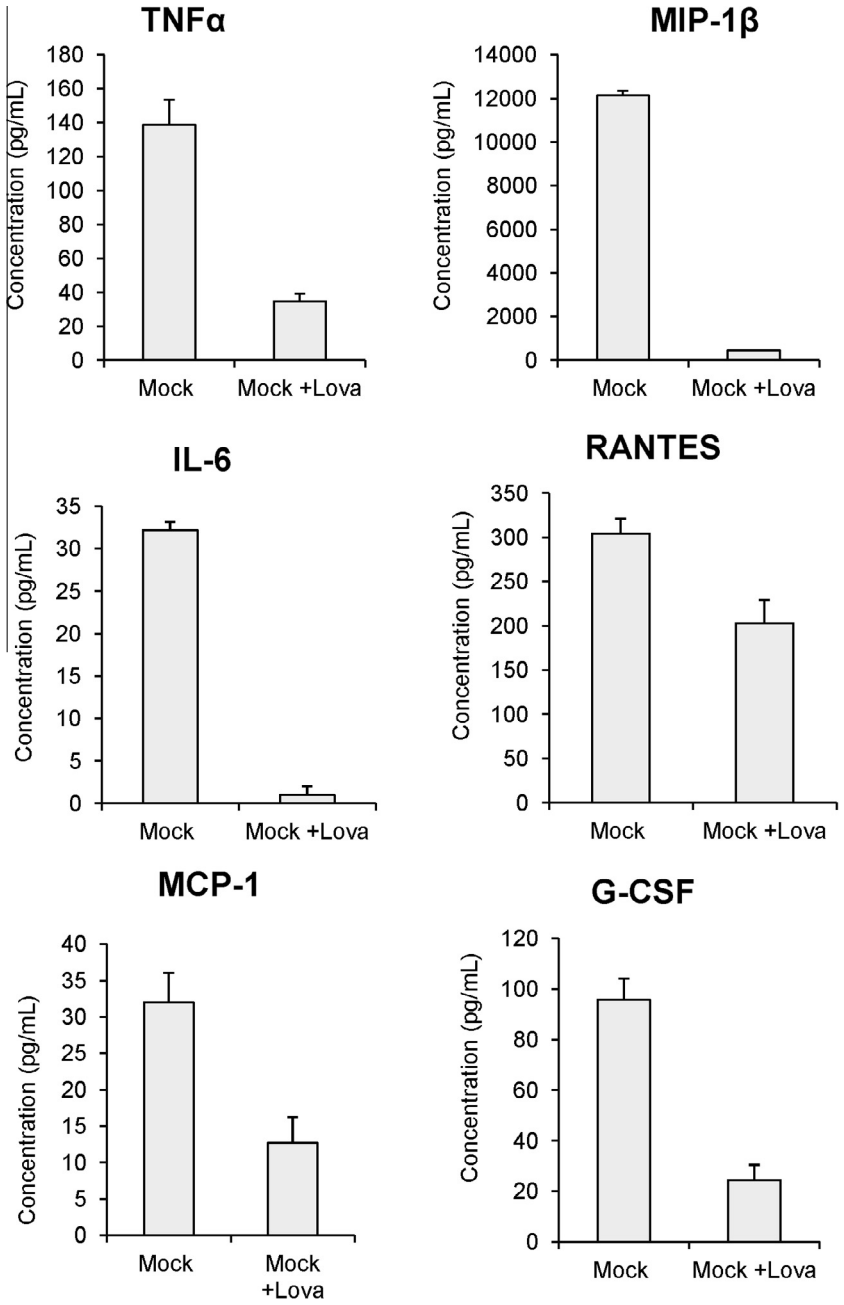

Fig. 6. The effect of lovastatin treatment on pro-inflammatory cytokine secretion in mock-infected RAW cells. RAW cells were either non-treated or treated with lovastatin and at 36 h (the equivalent of 24 h post-infection) the cytokines levels were measured. Representative data from one of two independent experiments is presented, and the average values and standard error obtained from triplicate measurements ($p < 0.05$) are shown.

is consistent with previous *in vitro* studies on primary mouse and human lung macrophages indicating abortive infection in lung macrophages (Becker et al., 1991; Becker et al., 1992; Franke-Ullmann et al., 1995).

3.2. Pro-inflammatory response in RSV-infected RAW cells

The host response to RSV infection in RAW cells was examined by measuring the changes in cytokine gene expression following virus infection. The mRNA levels of specific cytokines in mock-infected and virus-infected cells were compared using PCR array at 2 and 16 hpi. In general, either no increase or relatively small increases in mRNA levels of these cytokines were observed at 2 hpi, however at 16 hpi significantly higher cytokine gene expression levels was detected. Increased expression levels of MCP-1, MIP1β, TNFα, IL-6, G-CSF, RANTES (CXCL5) and CXCL10 was observed (Fig. 3A), although the magnitude of this increase was cytokine-specific (e.g. 10-fold (TNF) and 1000-fold (G-CSF3)).

The Bio-Plex Mouse Cytokine 23-Plex Panel was used to measure the levels of selected secreted cytokines in the tissue culture supernatant (TCS) of RSV-infected RAW cells (Fig. 3B) at between 4 and 24 hpi. A comparison of the cytokine levels in mock-infected cells and infected cells at 24 hpi showed significant increases in MCP-1, G-CSF, RANTES, TNFα, IL-6, and MIP-1β. These cytokines have been reported in lungs of RSV-infected mice and their human homologues have also been implicated in human disease severity (McNamara et al., 2005; Collins and Graham, 2008). In general a temporal increase in cytokine levels was observed from 8 hpi, with the largest increase occurring in a cytokine-specific manner at between 12 and 24 hpi. Some cytokines reached maximal levels at

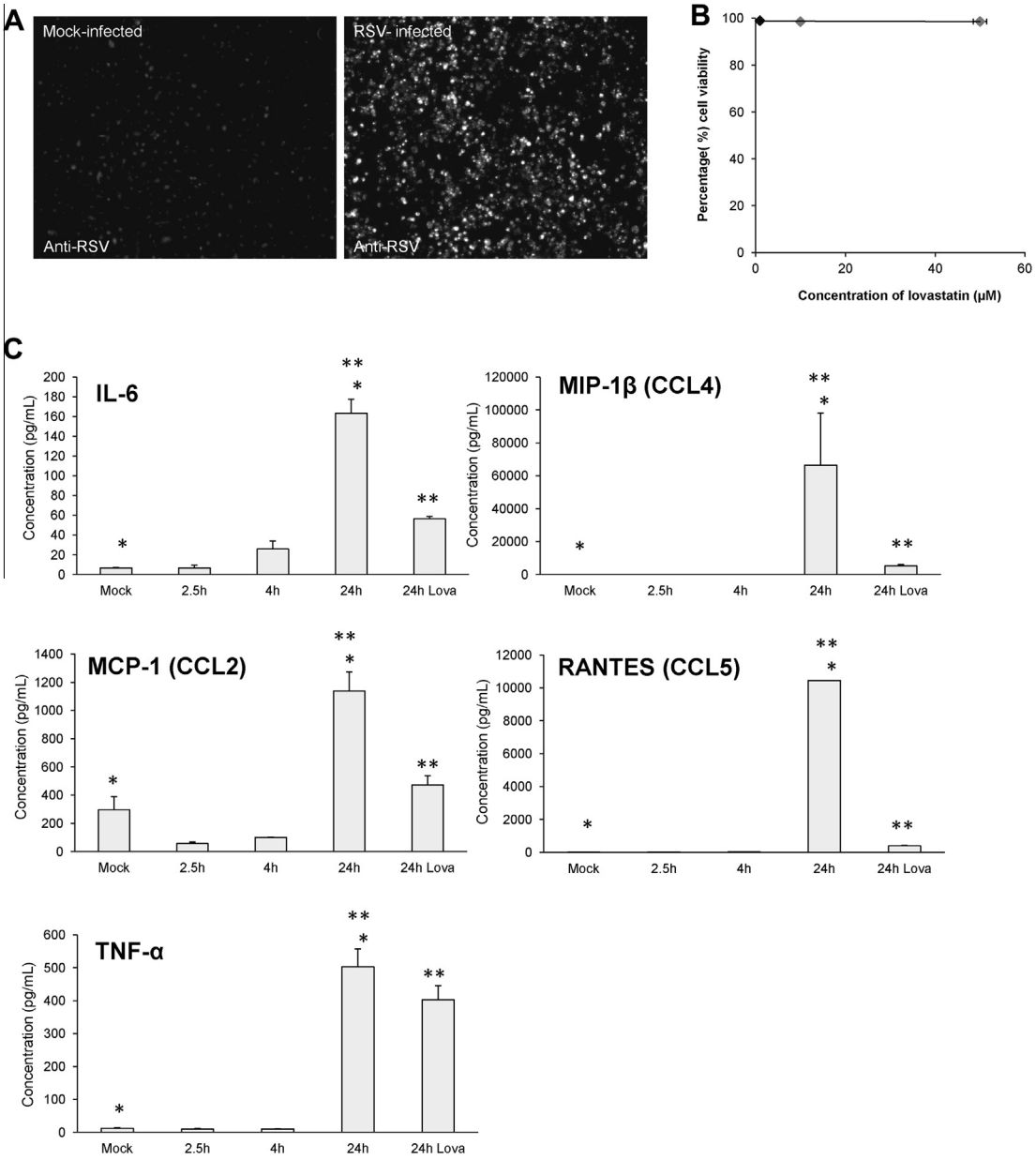

Fig. 7. The effect of lovastatin treatment on pro-inflammatory cytokine secretion in RSV-infected primary pulmonary murine macrophages. (A) Mock-infected and RSV-infected primary pulmonary murine macrophage cells were fixed at 24 h post-infection (hpi) and stained with anti-RSV. The stained cells were imaged by IF microscopy (objective ×10). (B) Mock-infected primary lung macrophage cells were incubated with increasing lovastatin concentrations for 28 h and the cell viability measured. Representative data from one of two independent experiments is presented, and the average values and standard error obtained from triplicate measurements ($p < 0.05$) are shown. (C) The cytokine concentrations were measured in the tissue culture supernatant of mock-infected, RSV-infected and lovastatin-treated RSV-infected primary lung macrophage cells at 24 hpi. Representative data from one of two independent experiments is presented, and the average values and standard error obtained from triplicate measurements are shown. (∗ and ∗∗ indicate pair wise comparisons $p < 0.05$).

12 hpi, after which the levels slightly declined (e.g. TNF and IL-6), while the G-CSF, MCP-1 and MIP-1β levels did not significantly increase after 12 hpi. In contrast, the RANTES levels appeared to continually increase up until 24 hpi. We also noted that several non-macrophage associated cytokines that are included in the Bio-Plex Mouse Cytokine 23-Plex Panel (e.g. Il4, IL5) were present at less than 25 ng/ml in either mock-infected or RSV-infected cells (Ravi Iyer and Sugrue, unpublished observations).

3.3. Lovastatin mitigates the pro-inflammatory response in RSV-infected macrophage cells

Statins have anti-inflammatory properties and previous studies have shown that lovastatin treatment was effective in protecting mice from lethal RSV infection (Gower and Graham, 2001). We therefore examined the effect of lovastatin treatment on pro-inflammatory cytokine secretion in RSV-infected RAW cells. No significant cell toxicity between 1 and 10 μM lovastatin was detected (Fig. 4A), and in all subsequent experiments cells were treated with 10 μM lovastatin. In non-treated and lovastatin-treated RSV-infected cells we observed similar numbers of RSV infected cells (Fig. 4B), M2-1 protein levels (Fig. 4C), and inclusion bodies (Fig. 4D), indicating that drug treatment did not inhibit virus infection. Furthermore, lovastatin treatment did not result in a significant reduction in cholesterol levels (unpublished observations).

Virus infection induced changes in the F-actin staining pattern (Fig. 5A), but immunoblotting using anti-actin indicated similar actin levels in non-treated and lovastatin-treated infected cells

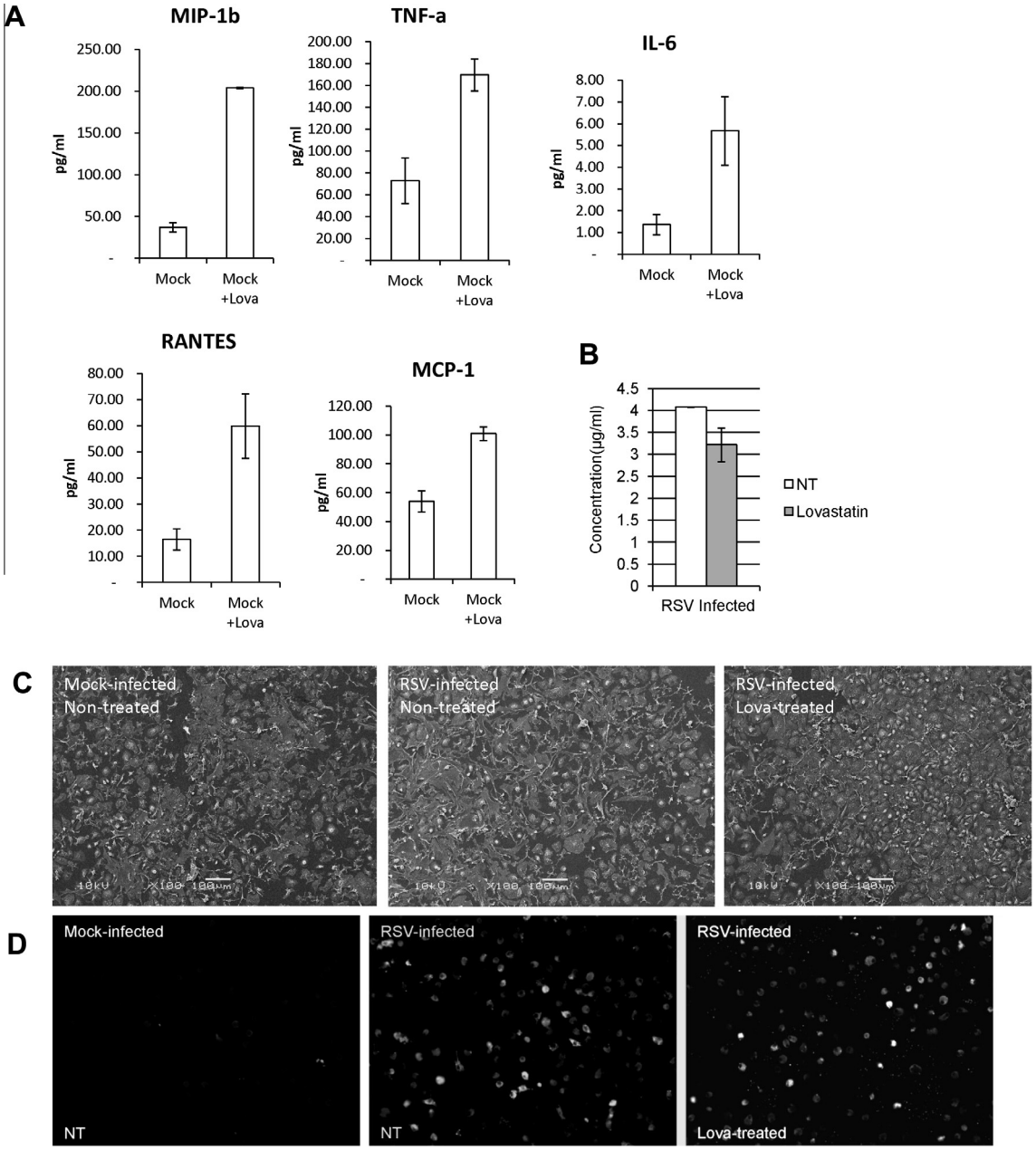

Fig. 8. The effect of lovastatin treatment on pro-inflammatory cytokine secretion in mock-infected primary pulmonary murine macrophages. (A) Cells were either non-treated or treated with lovastatin and at 36 h (the equivalent of 24 h post-infection) the cytokines levels were measured. Representative data from one of two independent experiments is presented, and the average values and standard error obtained from triplicate measurements ($p < 0.05$) are shown. Effect of lovastatin (Lova) on RSV-infected macrophage cells. (B) The cholesterol levels were measured in non-treated (NT) or Lovastatin-treated (Lovastatin) virus-infected cells at 24 h post-infection (hpi). Representative data obtained from two independent experiments is shown. The values represent the average of triplicate measurements ($p < 0.05$). (C) The macrophage cell morphology examined and compared in mock-infected and virus-infected cells either non-treated (NT) or lovastatin-treated (Lova-treated) cells using SEM (magnification × 100) at 24 hpi. **(D)** Mock-infected and RSV-infected cells either non-treated (NT) or lovastatin-treated (Lova-treated) were stained at 24 hpi using anti-RSV and imaged using fluorescence microscopy (objective ×10).

(Fig. 5B). However, this change was not observed in lovastatin-treated infected cells, indicating that lovastatin prevented this virus induced change. The cytokine levels in the TCS of non-treated and lovastatin-treated cells were measured at 24 hpi using the Bio-Plex Mouse Cytokine 23-Plex Panel. We noted a reduction of between 75% and 99% in the levels of IL6, MCP-1, RANTES, MIP1β, TNFα and G-CSF in lovastatin-treated RSV-infected cells compared to the non-treated cells (Fig. 5C). In mock-infected cells we noted very low cytokine levels at 24 hpi, and lovastain treatment produced a small reduction in these basal cytokine levels (Fig. 6).

The effect of lovastatin treatment on primary murine macrophages isolated from whole lung tissue was also examined. Staining of mock-infected and RSV-infected cells using anti-RSV showed staining in >95% of the infected cells (Fig. 7A). However, we noted that after 24 hpi these cells yielded a virus titer of 1.6×10^2 pfu/ml, suggesting inefficient progeny virus production. Similarly, pre-treatment of these cells with 10 μM lovastatin showed no significant cytotoxic effects under our experimental conditions (Fig. 7B). At 24 hpi the cytokine levels in the TCS of mock-infected and virus-infected pulmonary macrophages were measured

(Fig. 7C). Virus infection resulted in significant increase in RANTES, MCP-1, IL6, TNFα and MIP-1β levels by 24 hpi. Although lovastatin treatment caused a modest reduction in TNFα levels (~10%), other cytokines showed reduced levels of between 60% (e.g. IL6) and 99% (e.g. RANTES), similar to that observed in RSV-infected RAW cells.

Mock-infected cells showed a basal level of cytokine production (up to 100 pg/ml), and in general mock-infected cells treated with lovastatin exhibited a small increase in these basal cytokine levels (Fig. 8A). Analysis of the cholesterol levels in non-treated and lovastatin-treated RSV-infected cells indicated that lovastatin did not reduce the cellular cholesterol levels (Fig. 8B). Similar cell numbers (Fig. 8C) and anti-RSV staining levels (Fig. 8D) were observed in both non-treated and lovastatin-treated RSV-infected cells, suggesting that lovastatin did not significantly alter cell viability nor prevent virus infection.

4. Conclusion

An increase in virus antigen and the presence of inclusion bodies in RSV-infected macrophages cells correlated with increased levels of several pro-inflammatory cytokines. Some of these have been implicated in increased disease severity in infected humans (McNamara et al., 2005), and we observed a similar spectrum of virus-induced cytokines in RAW cells and cultured RSV-infected primary pulmonary macrophages, and in murine alveolar macrophage cells following *in vitro* RSV infection (Ravi Iyer and Sugrue, unpublished observations). Although RAW cells may differ in some physiological aspects from the primary murine pulmonary macrophages, in regards to RSV infection and subsequent cytokine secretion they appear to behave similarly. This suggests that the signalling networks that lead to virus-induced cytokine expression are retained in RAW cells. A role for rho GTPase signalling in this process is suggested by the inhibitory effect of lovastatin on RSV-induced changes in F-actin structure that correlated with reduced cytokine levels.

RSV is an immune-pathogenic virus, and much of the disease associated with RSV infection is mediated via the pro-inflammatory response it elicits. Although RSV infection in the LRT is likely to involve several cell types in the lung, the role of macrophages in the host response has been demonstrated (Haeberle et al., 2002; Pribul et al., 2008; Reed et al., 2008). Statins are currently licensed drugs for the treatment of heart disease, but several studies have also shown that they suppress pro-inflammatory cytokine secretion (e.g. in Sakamoto et al., 2009). We have demonstrated the potential of statin-based drugs to mitigate the inflammatory response in RSV-infected macrophages. Our observations may therefore partly help to explain the observation that lovastatin treatment protects mice from lethal RSV infection (Gower and Graham, 2001).

Finally, there are logistical and ethical issues in obtaining sufficient human and murine primary macrophages for screening compounds with anti-inflammatory activity. RAW cells and primary macrophage cells behave similarly, both with respect to RSV infection and in the RSV-induced pro-inflammatory cytokine response. RAW cells may therefore represent a cost-effective assay system for high-throughput screening of chemical libraries to identify drugs to control RSV-induced inflammation.

Acknowledgments

We acknowledge funding support by the Singapore MIT Alliance for Research and Technology (SMART). Laxmi Iyer Ravi and Richard Sutejo are recipients of NTU PhD scholarships (Ministry of Education, Singapore).

References

Becker, S., Quay, J., Soukup, J., 1991. Cytokine (tumor necrosis factor, IL-6, and IL-8) production by respiratory syncytial virus-infected human alveolar macrophages. J. Immunol. 147, 4307–4312.

Becker, S., Soukup, J., Yankaskas, J.R., 1992. Respiratory syncytial virus infection of human primary nasal and bronchial epithelial cell cultures and bronchoalveolar macrophages. Am. J. Respir. Cell Mol. Biol. 6, 369–374.

Brown, M.S., Dana, S.E., Goldstein, J.L., 1973. Regulation of 3-Hydroxy-3-Methylglutaryl Coenzyme A Reductase Activity in Human Fibroblasts by Lipoproteins. Proc. Natl. Acad. Sci. 70, 2162–2166.

Cannon, M.J., 1987. Microplaque immunoperoxidase detection of infectious respiratory syncytial virus in the lungs of infected mice. J. Virol. Methods 16, 293–301.

Chaudhry, M.Z., Wang, J.H., Blankson, S., Redmond, H.P., 2008. Statin (Cerivastatin) protects mice against sepsis-related death via reduced proinflammatory cytokines and enhanced bacterial clearance. Surg. Infect. 9, 183–194.

Collins, P.L., Graham, B.S., 2008. Viral and host factors in human respiratory syncytial virus pathogenesis. J. Virol. 82, 2040–2055.

Ferro, D., Parrotto, S., Basili, S., Alessandri, C., Violi, F., 2000. Simvastatin inhibits the monocyte expression of proinflammatory cytokines in patients with hypercholesterolemia. J. Am. Coll. Cardiol. 36, 427–431.

Franke-Ullmann, G., Pfortner, C., Walter, P., Steinmuller, C., Lohmann-Matthes, M., Kobzik, L., Freihorst, J., 1995. Alteration of pulmonary macrophage function by respiratory syncytial virus infection in vitro. J. Immunol. 154, 268–280.

Garcia, J., Garcia-Barreno, B., Vivo, A., Melero, J.A., 1993. Cytoplasmic inclusions of respiratory syncytial virus-infected cells: formation of inclusion bodies in transfected cells that coexpress the nucleoprotein, the phosphoprotein, and the 22K protein. Virology 195, 243–247.

Gower, T.L., Graham, B.S., 2001. Antiviral activity of lovastatin against respiratory syncytial virus in vivo and in vitro. Antimicrob. Agents Chemother. 45, 1231–1237.

Haeberle, H.A., Takizawa, R., Casola, A., Brasier, A.R., Dieterich, H.J., Van Rooijen, N., Gatalica, Z., Garofalo, R.P., 2002. Respiratory syncytial virus-induced activation of nuclear factor-kappaB in the lung involves alveolar macrophages and toll-like receptor 4-dependent pathways. J. Infect. Dis. 186, 1199–1206.

Huang, K.-C., Chen, C.-W., Chen, J.-C., Lin, W.-W., 2003. Statins induce suppressor of cytokine signaling-3 in macrophages. FEBS Lett. 555, 385–389.

Jeffree, C.E., Rixon, H.W., Brown, G., Aitken, J., Sugrue, R.J., 2003. Distribution of the attachment (G) glycoprotein and GM1 within the envelope of mature respiratory syncytial virus filaments revealed using field emission scanning electron microscopy. Virology 306, 254–267.

Johnson, J.E., Gonzales, R.A., Olson, S.J., Wright, P.F., Graham, B.S., 2007. The histopathology of fatal untreated human respiratory syncytial virus infection. Mod. Pathol. 20, 108–119.

Keyomarsi, K., Sandoval, L., Band, V., Pardee, A.B., 1991. Synchronization of tumor and normal cells from G1 to multiple cell cycles by lovastatin. Cancer Res. 51, 3602–3609.

Low, K.-W., Tan, T., Ng, K., Tan, B.-H., Sugrue, R.J., 2008. The RSV F and G glycoproteins interact to form a complex on the surface of infected cells. Biochem. Biophys. Res. Commun. 366, 308–313.

McDonald, T.P., Pitt, A.R., Brown, G., Rixon, H.W.M., Sugrue, R.J., 2004. Evidence that the respiratory syncytial virus polymerase complex associates with lipid rafts in virus-infected cells: a proteomic analysis. Virology 330, 147–157.

McNamara, P.S., Flanagan, B.F., Hart, C.A., Smyth, R.L., 2005. Production of Chemokines in the Lungs of Infants with Severe Respiratory Syncytial Virus Bronchiolitis. J. Infect. Dis. 191, 1225–1232.

Nair, H., Nokes, D.J., Gessner, B.D., Dherani, M., Madhi, S.A., Singleton, R.J., O'Brien, K.L., Roca, A., Wright, P.F., Bruce, N., Chandran, A., Theodoratou, E., Sutanto, A., Sedyaningsih, E.R., Ngama, M., Munywoki, P.K., Kartasasmita, C., Simões, E.A.F., Rudan, I., Weber, M.W., Campbell, H., 2010. Global burden of acute lower respiratory infections due to respiratory syncytial virus in young children: a systematic review and meta-analysis. Lancet 375, 1545–1555.

Novack, V., Eisinger, M., Frenkel, A., Terblanche, M., Adhikari, N., Douvdevani, A., Amichay, D., Almog, Y., 2009. The effects of statin therapy on inflammatory cytokines in patients with bacterial infections: a randomized double-blind placebo controlled clinical trial. Intensive Care Med. 35, 1255–1260.

Osborne, T.F., Gil, G., Brown, M.S., Kowal, R.C., Goldstein, J.L., 1987. Identification of promoter elements required for in vitro transcription of hamster 3-hydroxy-3-methylglutaryl coenzyme a reductase gene. Proc. Natl. Acad. Sci. USA 84, 3614–3618.

Perrone, L.A., Plowden, J.K., Garcia-Sastre, A., Katz, J.M., Tumpey, T.M., 2008. H5N1 and 1918 pandemic influenza virus infection results in early and excessive infiltration of macrophages and neutrophils in the lungs of mice. PLoS Pathog. 4, e1000115.

Pribul, P.K., Harker, J., Wang, B., Wang, H., Tregoning, J.S., Schwarze, J., Openshaw, P.J., 2008. Alveolar macrophages are a major determinant of early responses to viral lung infection but do not influence subsequent disease development. J. Virol. 82, 4441–4448.

Radhakrishnan, A., Yeo, D., Brown, G., Myaing, M.Z., Iyer, L.R., Fleck, R., Tan, B.H., Aitken, J., Sanmun, D., Tang, K., Yarwood, A., Brink, J., Sugrue, R.J., 2010. Protein analysis of purified respiratory syncytial virus particles reveals an important role for heat shock protein 90 in virus particle assembly. Mol. Cell. Proteomics 9, 1829–1848.

Reed, J.L., Brewah, Y.A., Delaney, T., Welliver, T., Burwell, T., Benjamin, E., Kuta, E., Kozhich, A., McKinney, L., Suzich, J., Kiener, P.A., Avendano, L., Velozo, L., Humbles, A., Welliver, R.C., Coyle, A.J., 2008. Macrophage impairment underlies airway occlusion in primary respiratory syncytial virus bronchiolitis. J. Infect. Dis. 198, 1783–1793.

Rezaie-Majd, A., Maca, T., Bucek, R.A., Valent, P., Muller, M.R., Husslein, P., Kashanipour, A., Minar, E., Baghestanian, M., 2002. Simvastatin reduces expression of cytokines interleukin-6, interleukin-8, and monocyte chemoattractant protein-1 in circulating monocytes from hypercholesterolemic patients. Arterioscler. Thromb. Vasc. Biol. 22, 1194–1199.

Sakamoto, N., Hayashi, S., Mukae, H., Vincent, R., Hogg, J.C., van Eeden, S.F., 2009. Effect of atorvastatin on PM10-induced cytokine production by human alveolar macrophages and bronchial epithelial cells. Int. J. Toxicol. 28, 17–23.

Sugrue, R.J., Brown, C., Brown, G., Aitken, J., McL. Rixon, H.W., 2001. Furin cleavage of the respiratory syncytial virus fusion protein is not a requirement for its transport to the surface of virus-infected cells. J. Gen. Virol. 82, 1375–1386.